# Uniaxial Magnetic Anisotropy in Nanostructured Co/Cu(001): From Surface Ripples to Nanowires

R. Moroni,[1,2] D. Sekiba,[1] F. Buatier de Mongeot,[1,*] G. Gonella,[1,2] C. Boragno,[1] L. Mattera,[1,2] and U. Valbusa[1]

[1]*Unità INFM di Genova, Dipartimento di Fisica dell'Università di Genova, via Dodecaneso 33, I-16146 Genova, Italy*

[2]*IMEM-CNR Sezione di Genova, via Dodecaneso 33, I-16146 Genova, Italy*

(Received 28 February 2003; published 17 October 2003)

We have investigated the correlation between morphology and magnetic anisotropy in nanostructured Co films on Cu(001). The formation of nanoscale ripples by ion erosion is found to deeply affect the magnetic properties of the Co film. A surface-type uniaxial magnetic anisotropy with easy axis parallel to the ripples is observed. The origin of the magnetic anisotropy has been identified with the modification of thermodynamic-step distribution induced by ripple formation. At higher ion doses, when Co ripples detach and crystalline nanowires form, a strong enhancement of the magnetic anisotropy due to magnetostatic contributions is observed.

DOI: 10.1103/PhysRevLett.91.167207 PACS numbers: 75.30.Gw, 75.75.+a, 68.37.Ef, 81.16.Rf

In recent years, assembling and characterization of nanometer-sized structures have attracted a great deal of interest, and demonstrated that their magnetic properties can be drastically different from those of bulk materials [1]. With the decreasing size of magnetic systems, surface contributions to magnetic anisotropy, which are related to the undercoordination of atoms at the interface, become more and more relevant. In nanosized objects, except for highly symmetric cluster shapes [2,3], interface effects may dominate the overall magnetic anisotropy. In ultrathin films, it can be expected that the symmetry reduction which follows the creation of nanoscale surface patterns deeply affects the magnetic anisotropy. Experiments on ferromagnetic transition-metal films deposited on vicinal surfaces have shown a strict correlation between morphology and magnetism and, in particular, that atomic steps may be a source of magnetic anisotropy [4]. Nevertheless, once we depart from the ideal case of a regularly stepped surface and deal with nanostructured films characterized by complex profiles [5], the understanding of the origin of magnetic anisotropy is complicated by the interplay of different effects, as surface and magnetostatic contributions. Experimentally, the separation of the different contributions would benefit from the possibility of monitoring magnetic properties while varying the morphology of nanostructured films in a controlled way. Recently, ion induced nanostructuring was demonstrated to be a powerful method to induce self-organized nanoscale patterns [6]. In particular, it was found that sputtering at grazing incidence and low temperature induces the formation of crystalline nanoscale ripples oriented parallel to the ion beam projection independently from the symmetry of the substrate. Moreover, by varying the ion dose, it is possible to finely tune the ripple wavelength and depth and, above all, the nonequilibrium step distribution which, as a consequence of ripple formation, is dramatically unbalanced parallel to the ripple ridges [7].

In this Letter, we investigate the correlation between morphology and magnetic anisotropy in nanostructured Co films on Cu(001). Film morphology and magnetic anisotropy have been deduced from scanning tunneling microscopy (STM) and magneto-optical Kerr effect (MOKE) measurements. The ability to tune the morphology of nanoscale artificial patterns by means of ion sculpting is combined with the quantitative determination of magnetic anisotropy and allows one to determine the relative importance of surface and magnetostatic contributions. The formation of nanoscale Co ripples reduces the fourfold symmetry of fcc Co to uniaxial and correspondingly a strong in-plane uniaxial magnetic anisotropy parallel to the ripple axis develops. In the early stages of ripple formation, the observed surface-type magnetic anisotropy is induced by the unbalance of the thermodynamic-step distribution in favor of monatomic steps parallel to ripple ridges. At a higher ion dose, when ripple troughs are etched as far as the Cu substrate and crystalline nanowires of Co are formed, a strong enhancement of the magnetic anisotropy due to magnetostatic contributions occurs.

The Cu(001) substrate was prepared by cycles of 1 keV $Ar^+$ sputtering and annealing at 800 K. After such a procedure the substrate exhibited a sharp LEED pattern and STM images revealed an average terrace size of about 100 nm while all contaminants were found below Auger-electron spectroscopy (AES) detection sensitivity. Cobalt films have been evaporated at normal incidence on the substrate held at 300 K. The deposition rate and Co coverage were determined by STM and quantitative AES.

According to the quasi-ideal layer-by-layer growth mode observed for Co films on Cu(001) at $T = 300$ K [8], after the deposition of 12 monolayer equivalents (MLE) of Co referenced to the Cu(001) surface density (1 MLE $\sim$ 15.3 atoms/nm$^2$), five layers are exposed [Fig. 1(a)] and the rms interface width is about 0.17 nm. An equivalent distribution of steps along the symmetric [110] and [1-10] directions is found to bound the Co islands. Such step termination is thermodynamically favored and, as shown in Fig. 1(b), longitudinal MOKE

  

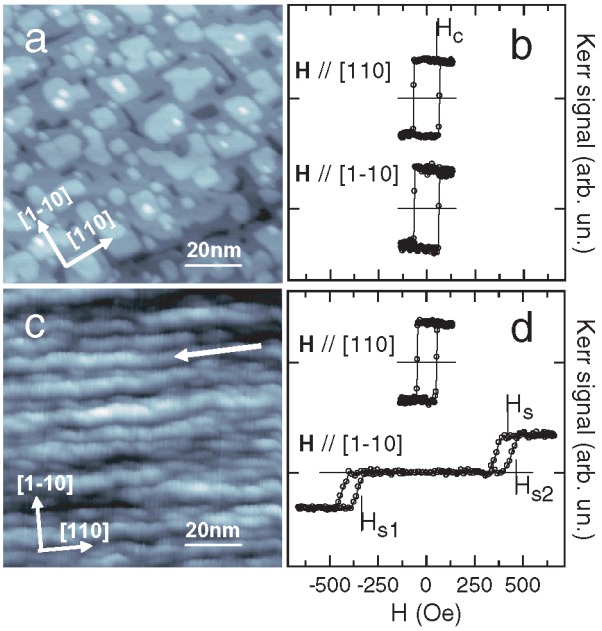


FIG. 1 (color online). (a) STM image and (b) hysteresis curves of the flat 12 MLE thick Co/Cu(001) film. (c) STM image and (d) hysteresis curves of the Co film after nanostructuring with an ion dose of about 12 MLE. The arrow indicates the projection on the surface plane of the ion beam direction.

measurements indicate that the two directions are equivalent also from a magnetic point of view. Patterning of the Co films was achieved by sputtering at an incidence angle of 70° from the normal to the surface along the close-packed [110] azimuthal direction with a defocused $Ar^+$ ion beam at 1 keV. The ion current on the sample was 2 $\mu$A which corresponds to an ion dose of about $1.6 \times 10^{-2}$ MLE per second. The sample temperature was kept at 180 K during sputtering and then rapidly lowered down to 140 K in order to reduce adatom diffusion and inhibit surface reorganization. STM and MOKE measurements were both performed at 140 K. As shown in Fig. 1(c), sputtering in the above described conditions leads to the formation of ripple structures elongated along the [110] direction, i.e., parallel to the ion beam projection, with a lateral periodicity in the range of 10 nm. These results demonstrate that in ultrathin Co/Cu(001) films, ion sculpting produces nanostructures which are closely analogous to the ones found in single-crystal metal surfaces [6], where the envelope of the ripple is formed by a regular staircase of narrow terraces separated by monatomic steps whose edges run along the ripple ridges [7]. In this regime of ion erosion the line profile across the ripple is properly described by a triangular waveform and the ripple sides are found to form well-defined facets as demonstrated by surface diffraction experiments [9].

Atomic steps along the ⟨110⟩ directions are known to be a source of magnetic anisotropy as demonstrated by experiments performed on Co films deposited on miscut Cu(001) substrates where the unbalance between the density of [110] and [1-10] steps induces an in-plane uniaxial anisotropy [10]. For that reason, the results of Fig. 1(c) are particularly intriguing as they demonstrate that ion induced nanostructuring allows one to produce in a controlled way artificial nonthermodynamic surface profiles and to strongly unbalance the density of steps along the projection of the ion beam. As expected, the magnetic measurements of Fig. 1(d) indeed reveal that a strong uniaxial in-plane magnetic anisotropy develops with the easy axis parallel to the ripples. Following ion sputtering and ripple formation, the hysteresis curve along the [1-10] direction (i.e., with the magnetic field perpendicular to the ripple axis) splits into two semiloops. The origin of the hysteresis-curve modification is the change of the magnetization switching process [11]. For sufficiently high applied magnetic fields, the sample magnetization is saturated along the magnetic field as shown by the non-null and saturated Kerr signal. When the applied magnetic field is reversed, the Kerr signal is null for a large interval between $H_{s1}$ and $H_{s2}$ which means that, in this magnetic field range, the magnetization direction is pinned along the easy axis [Fig. 1(d)]. Both $H_{s1}$ and $H_{s2}$ are much larger than the coercive field $H_c$ indicating that the magnetization switching process has been strongly modified by the large uniaxial magnetic anisotropy induced by the ripple structure. Despite such a strong modification, sharp irreversible transitions were observed in the whole ion-dose range, indicating that domain nucleation plays a minor role in the magnetization switching process. Since defects can act as nucleation sites, the observation of sharp irreversible transitions indicates that the nanostructured Co film has a good crystalline quality as independently confirmed by experiments on single-crystal metal surfaces [7,12].

In order to delve deeper into the correlation between ripple morphology and uniaxial magnetic anisotropy, their evolution was investigated as a function of the ion dose. From the STM images one can extract the ripple wavelength $\Lambda$ and the rms interface width $w$. In Fig. 2, the dependence of $\Lambda$ and $w$ on the ion dose $\Phi$ is shown. In close analogy to the already cited experiments on single-crystal metal surfaces, the measured trend of wavelength and interface width is well described by a power law behavior as $\Lambda = a\Phi^z$ and $w = w_0 + b\Phi^\beta$ where $w_0$ is the initial roughness [6]. Such an analysis allows one to determine the scaling exponents $z = 0.08 \pm 0.01$ and $\beta = 0.53 \pm 0.09$ and the prefactors $a = 6.57 \pm 0.16$ nm and $b = 0.03 \pm 0.005$ nm. Quantitative information about magnetic anisotropy can be extracted from the measured hysteresis curves by introducing the shift field $H_s = (H_{s2} - H_{s1})/2$ which is directly related to the uniaxial anisotropy constant $K_u$ through $K_u = M_s H_s$ where $M_s$ is the saturation magnetization [11]. As shown in Fig. 3(a), in the evolution of $H_s$ two distinct regimes can be identified. In the early stages of ion nanostructuring a uniaxial anisotropy suddenly develops and grows with the ion dose [region I in Fig. 3(a)]. After the initial

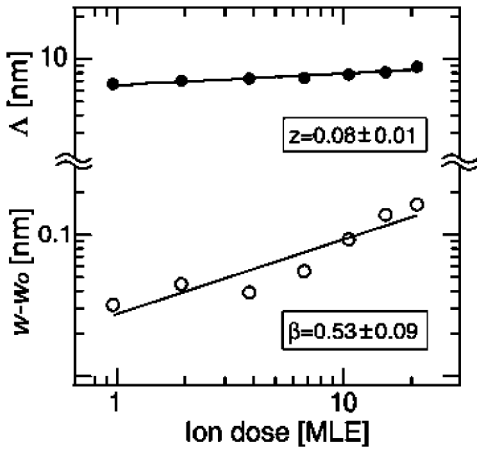


FIG. 2. The scaling law of the ripple wavelength $\Lambda$ (●) and the rms interface width $w$ (○) with respect to the ion dose $\Phi$.

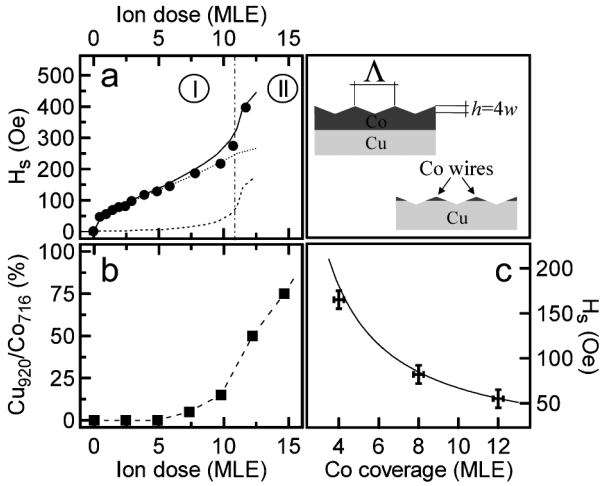


FIG. 3. (a) Experimental shift field $H_s$ (●) as a function of the ion dose $\Phi$ compared to the calculated magnetostatic (dashed line) and Néel (dotted line) contributions to magnetic anisotropy. The continuous line shows the sum of the two terms. (b) $Cu_{920}$ to $Co_{716}$ Auger-peak-intensity ratio (■) as a function of the ion dose $\Phi$. (c) Shift fields $H_s$ as a function of the initial Co coverage $t$ after nanostructuring with an ion dose of 1 MLE. The continuous line has been calculated by means of Eq. (1a).

smooth growth, a sudden steeper increase in $H_s$ is observed, followed by the decay of the Kerr signal up to its disappearance [region II in Fig. 3(a)]. Such a discontinuous behavior of $H_s$ at 11 MLE while surface morphology evolves smoothly (Fig. 2) may be associated with the onset of ripple detachment since the Cu to Co Auger-peak intensity ratio correspondingly increases [Fig. 3(b)]. Despite nanowire formation, magnetization reversal mainly proceeds via domain-wall motion and the shift field can be extracted by hysteresis loops as shown in Fig. 1(d).

In order to quantitatively describe the evolution of magnetic anisotropy, we adopt a phenomenological model which takes into account step-induced and magnetostatic contributions to the magnetic anisotropy. Because of the large aspect ratio of ripples [Fig. 1(c)], a one-dimensional model has been implemented which takes into account the surface profile perpendicular to the ripple ridges. The contributions from the atoms at step sites have been considered in the frame of the nearest-neighbor Néel pair-bonding model [13] while no contribution from bulk and terrace atoms has been included [10]. In order to evaluate the surface contribution to the anisotropy, the density of atoms at [110]-step sites was derived from the ripple envelope which is well described by a triangular waveform where the side facets consist of a regular staircase of terraces separated by monatomic [110] steps (inset of Fig. 3). The density of steps is therefore derived in a straightforward manner by the ripple wavelength $\Lambda$ and the ripple height $h$ which is related to the rms roughness $w$ derived from STM images [14]. By making these assumptions, the uniaxial anisotropy constant expressed in terms of the shift field $H_s$ as a function of the ion dose reads

$$H_s = \frac{A\Phi^{\beta-z}}{t - S_y\Phi}, \quad \text{if } \Phi < \Phi_d, \tag{1a}$$

$$H_s = \frac{2A\Phi^{\beta-z}}{t - S_y\Phi + (t - S_y\Phi_d)(\frac{\Phi}{\Phi_d})^{\beta}}, \quad \text{if } \Phi > \Phi_d. \tag{1b}$$

In Eq. (1), $A$ is related to the anisotropy energy per atom at step site $E_a$ by $A = (E_a/M_s)(32\sqrt{2}/c^3)(b/a)$ where $c$ is the lattice constant of the Co film, $b$ is the prefactor of the power law for the roughness, and $a$ is that of the wavelength power law. The exponent $\beta - z$, where $\beta$ and $z$ are the exponents of the power law dependence of the roughness and the ripple wavelength on the ion dose, derives from the fact that $h/\Lambda$ gives the number of steps along the [110] direction (i.e., parallel to the ripple axis) per unit surface area. The denominator in Eq. (1a), where $S_y$ is the sputtering yield of Co, takes into account the surface-type behavior of the anisotropy which originates from atoms at step sites. Finally, $t$ is the initial Co coverage and $\Phi_d$ is the ion dose at which Co wires detach. Equation (1) holds if $\Phi$ and $t$ are expressed in adimensional MLE units.

The magnetostatic contribution to the anisotropy has been evaluated by performing micromagnetic calculations [15]. In analogy with the evaluation of the Néel contribution, a triangular ripple envelope deduced by the STM data has been considered and $\Phi_d$ was set equal to 11 MLE. Since the ripple width ($\Lambda \sim 8$ nm) is of the order of the magnetostatic exchange length ($L \sim 7$ nm), an almost uniform magnetization lying in the (001) planes, which is also favored by magnetocrystalline anisotropy, has been found even when the magnetization is perpendicular to the ripples. For this magnetization direction, at the ripple sidewalls there exist uncompensated magnetic poles generating a demagnetizing field which is directed antiparallel and parallel to the magnetization, respectively, beneath ripple ridges and troughs. For low ion

doses ($\Phi < \Phi_d$), until ripples are connected, the contributions of these two regions to magnetostatic energy partly compensate resulting in a smooth increase in shape anisotropy. At ripple detachment, where the ion beam starts carving the Cu substrate and disconnected Co nanowires form (inset of Fig. 3), the shape anisotropy strongly increases. The micromagnetic calculations allow one to evaluate the sharp increase in shape anisotropy across ripple disconnection and its evolution before detachment. Quantitative agreement between calculation and experiment is obtained by reducing the calculated shape anisotropy by a factor of 3, a reduction which might be induced by uncorrelated roughness which is not taken into account in the calculations [16]. By making this assumption, at 10 MLE the shape anisotropy contributes to the overall anisotropy less than 15% and a negligible contribution is found below 8 MLE. We will therefore disregard the shape anisotropy contribution in region I.

For $\Phi < \Phi_d$, the shift field measured as a function of the ion dose for a 12 ML thick Co film was fitted by means of Eq. (1a) in which $A$, $\beta - z$, and $S_y$ were used as fitting parameters. The best agreement, which is shown in Fig. 3(a), was obtained with $A = 640 \pm 30$ Oe, $\beta - z = 0.41 \pm 0.07$, and $S_y = 0.5 \pm 0.1$. The value of $A$ corresponds to an anisotropy energy per atom at a step site of about $1.4 \times 10^{-4}$ eV which is of the order of the value obtained by the Néel pair-bonding model ($0.7 \times 10^{-4}$ eV [13]). The value of $\beta - z$ agrees very well with that obtained from the STM results shown in Fig. 2 ($\beta_{\mathrm{STM}} - z_{\mathrm{STM}} = 0.45 \pm 0.1$) and $S_y$ turns out to match well with the sputtering yield reported for Co sputtered with 1 keV $Ar^+$ ions [17]. In Fig. 3(a), the Néel and magnetostatic contributions to magnetic anisotropy are shown together with their sum. The agreement between the observed experimental trend and the phenomenological model presented here allows one to attribute the origin of the abrupt increase in $H_s$ to the detachment of Co ripples. At higher ion doses, the Kerr signal decays until it completely disappears, whereas AES still reveals the presence of Co on the sample. The disappearance of the long-range ferromagnetic order is probably related to ion induced intermixing which is expected to be important when a low Co coverage is left on the surface. As mentioned above, the magnetic anisotropy described by Eq. (1a) is of a surface type, which has been confirmed by measurements of the magnetic anisotropy at a fixed ion dose for different initial Co coverages [Fig. 3(c)]. The observed decrease of the magnetic anisotropy for increasing Co coverage is consistent with the surface-type behavior of the anisotropy and the measured $H_s$'s show a remarkable agreement with the ones calculated by means of Eq. (1a) as a function of $t$. This behavior is in contrast with the volume-type anisotropy found for Co films on vicinal Cu(001) surfaces [18]. A possible origin of such discrepancy might be related to the fact that in the present case, as shown by micromagnetic calculations, the magnetization is parallel to the (001) terraces, while in the case of vicinal surfaces is tilted towards the average optical plane [19].

The present results demonstrate that the surface contribution to the magnetic anisotropy of a nanostructured system enhances if its morphology is forced in a strongly nonequilibrium configuration. Indeed, experiments on magnetic nanoclusters which adopt equilibrium symmetric shapes find that the surface magnetic anisotropy tends to be averaged out [2,3]. We also stress that the remarkable agreement between the predicted evolution of the magnetic anisotropy and the STM determination of the nanostructure morphology allows the separation of the different contributions to the magnetic anisotropy. In particular, the experiment evidences how the dimensionality reduction in a nanostructured magnetic system from two dimensional (corrugated film) to one dimensional (disconnected wires) has a dramatic impact on the magnetostatic contribution to the magnetic anisotropy.

We acknowledge financial support from the MIUR-FIRB programs RBNE017XSW and RBNE01YLKN.

*Corresponding author.
Email address: buatier@fisica.unige.it

[1] J. Shen and J. Kirschner, Surf. Sci. **500**, 300 (2002).
[2] M. Jamet *et al.*, Phys. Rev. Lett. **86**, 4676 (2001).
[3] D. A. Garanin and H. Kachkachi, Phys. Rev. Lett. **90**, 065504 (2003).
[4] A. Berger, U. Linke, and H. P. Oepen, Phys. Rev. Lett. **68**, 839 (1992); J. Chen and J. L. Erskine, *ibid.* **68**, 1212 (1992); R. K. Kawakami, E. J. Escorcia-Aparicio, and Z. Q. Qiu, *ibid.* **77**, 2570 (1996).
[5] S. van Dijken, G. Di Santo, and B. Poelsema, Phys. Rev. B **63**, 104431 (2001).
[6] U. Valbusa, C. Boragno, and F. Buatier de Mongeot, J. Phys. Condens. Matter **14**, 8153 (2002).
[7] S. Rusponi *et al.*, Appl. Phys. Lett. **75**, 3318 (1999).
[8] U. Ramsperger *et al.*, Phys. Rev. B **53**, 8001 (1996).
[9] C. Boragno *et al.*, Phys. Rev. B **65**, 153406 (2002).
[10] R. K. Kawakami *et al.*, Phys. Rev. B **58**, R5924 (1998).
[11] R. P. Cowburn, S. J. Gray, and J. A. C. Bland, Phys. Rev. Lett. **79**, 4018 (1997).
[12] G. Costantini *et al.*, Phys. Rev. Lett. **86**, 838 (2001).
[13] D. S. Chuang, C. A. Ballentine, and R. C. O'Handley, Phys. Rev. B **49**, 15 084 (1994).
[14] For a triangular waveform $h = 4w$.
[15] The NIST-OOMMF code (http://math.nist.gov/oommf) was used to perform micromagnetic calculations.
[16] Y.-P. Zhao *et al.*, Phys. Rev. B **60**, 1216 (1999).
[17] V. S. Smentkowski, Prog. Surf. Sci. **64**, 1 (2000).
[18] P. Krams, B. Hillebrands, and G. Güntherodt, Phys. Rev. B **49**, 3633 (1994).
[19] Y. Z. Wu *et al.*, Phys. Rev. B **67**, 094409 (2003).